3358 (1967).
(16) H. Yamakawa, *J. Chem. Phys.*, **46**, 973 (1967).
(17) K. Okita, A. Teramoto, K. Kawahara, and H. Fujita, *J. Phys. Chem.*, **72**, 278 (1968).
(18) A. Dondos and H. Benoit, *J. Polym. Sci., Part B*, **7**, 335 (1969).
(19) P. Debye, *J. Phys. Chem.*, **51**, 18 (1947).
(20) B. H. Zimm, *J. Chem. Phys.*, **16**, 1093 (1948); **16**, 1099 (1948).
(21) H. Yamakawa, "Modern Theory of Polymer Solutions," Harper & Row, New York, N. Y., 1971, Chapter VII.
(22) H. Yamakawa, *Pure Appl. Chem.*, **31**, 179 (1972).
(23) W. H. Stockmayer and M. Fixman, *J. Polym. Sci., Part C*, **1**, 137 (1963).
(24) A. Yamamoto, M. Fujii, G. Tanaka, and H. Yamakawa, *Polym. J.*, **2**, 799 (1971).
(25) H. Shogenji, *Busseiron Kenkyu*, **62**, 1 (1953).
(26) T. Ooi, *J. Polym. Sci.*, **28**, 459 (1958).
(27) W. G. McMillan and J. E. Mayer, *J. Chem. Phys.*, **13**, 276 (1945).
(28) G. C. Berry, *J. Chem. Phys.*, **44**, 4550 (1966).
(29) P. J. Flory, "Principles of Polymer Chemistry," Cornell University Press, Ithaca, New York, N. Y., 1953, Chapter XIII.
(30) "International Critical Tables," Vol. III, E. W. Washburn, Ed., McGraw-Hill, New York, N. Y., 1928, pp 28, 29.
(31) G. Tanaka, S. Imai, and H. Yamakawa, *J. Chem. Phys.*, **52**, 2639 (1970).
(32) G. V. Schulz, O. Bodmann, and H.-J. Cantow, *J. Polym. Sci.*, **10**, 73 (1953).
(33) C. I. Carr and B. H. Zimm, *J. Chem. Phys.*, **18**, 1616 (1950).
(34) A. Živný, J. Pouchlý, and K. Solc, *Collect. Czech. Chem. Commun.*, **32**, 2753 (1967).
(35) J. M. G. Cowie and J. T. McCrindle, *Eur. Polym. J.*, **8**, 1185 (1972).
(36) H.-G. Elias and O. Etter, *Makromol. Chem.*, **66**, 56 (1963).
(37) A. Dondos and H. Benoit, *Eur. Polym. J.*, **4**, 561 (1968); **6**, 1439 (1970).
(38) T. Norisuye, K. Kawahara, A. Teramoto, and H. Fujita, *J. Chem. Phys.*, **49**, 4330 (1968).
(39) K. Kawahara, T. Norisuye, and H. Fujita, *J. Chem. Phys.*, **49**, 4339 (1968).
(40) K. Takashima, G. Tanaka, and H. Yamakawa, *Polym. J.*, **2**, 245 (1971).
(41) T. Matsumoto, N. Nishioka, and H. Fujita, *J. Polym. Sci., Part A-2*, **10**, 23 (1972).
(42) T. Tsuji and H. Fujita, *Polym. J.*, **4**, 409 (1973).
(43) P. J. Flory and W. R. Krigbaum, *J. Chem. Phys.*, **18**, 1086 (1950).
(44) T. A. Orofino and P. J. Flory, *J. Chem. Phys.*, **26**, 1067 (1957).
(45) P. J. Flory, *J. Chem. Phys.*, **17**, 303 (1949).
(46) W. H. Stockmayer, *Makromol. Chem.*, **35**, 54 (1960).
(47) M. Kurata, M. Fukatsu, H. Sotobayashi, and H. Yamakawa, *J. Chem. Phys.*, **41**, 139 (1964).
(48) H. Yamakawa, *J. Chem. Phys.*, **48**, 2103 (1968).
(49) H. Yamakawa and G. Tanaka, *J. Chem. Phys.*, **47**, 3991 (1967).

Light Scattering from Wormlike Chains. Determination of the Shift Factor

Hiromi Yamakawa* and Motoharu Fujii

Department of Polymer Chemistry, Kyoto University, Kyoto, Japan. *Received April 8, 1974*

ABSTRACT: The light-scattering form factor of wormlike chains without excluded volume is evaluated by the use of the Hermite polynomial expansion of the distribution function. The good convergence is obtained in the practically important range by taking account of the moments $\langle R^{2m} \rangle$ with m = 1-11. Evaluation of the latter is carried out by the operational method. The final results are obtained only numerically by the use of a digital computer. A method of determining the shift factor M_L and the Kuhn segment length λ^{-1} from light-scattering data is proposed. It is applied to DNA. The estimates of these parameters are then found to be in good agreement with those obtained previously from a comparison of viscosity and sedimentation.

In a previous paper,[1] a method on the assumption of a continuous wormlike model for stiff-chain macromolecules has been proposed for the determination of the shift factor M_L, as defined as the molecular weight per unit contour length, and of the Kuhn segment length λ^{-1} from a comparison of viscosity and sedimentation. The object of the present paper is to present a similar method of determining the same parameters from light-scattering measurements alone. It requires the light-scattering form factor $P(\theta)$.

For the wormlike chain, only approximate expressions for $P(\theta)$ have been derived by Peterlin,[2] Benoit and Doty,[3] Hearst and Harris,[4] Sharp and Bloomfield,[5] and many others; a complete list of the literature is found elsewhere.[6] Some of them are very poor in the typical stiff-chain region, and cannot be used to obtain correct estimates of the parameters. In particular, there is a controversy about the light-scattering estimate of the Kuhn segment length of DNA,[7-9] and it should be reexamined. Therefore, our first problem is to evaluate $P(\theta)$ exactly.

If all lengths are measured in units of λ^{-1}, the scattering factor for the chain of contour length L and without excluded volume is given by

$$P(\theta) = 2L^{-2} \int_0^L (L - t) I(\mathbf{k}; t) \mathrm{d}t \qquad (1)$$

where $I(\mathbf{k};t)$ is the characteristic function, or the Fourier transform of the distribution function of the end-to-end distance $\mathbf{R}$, for the chain of contour length t, and $\mathbf{k}$ is the scattering vector, whose magnitude is

$$k = (4\pi/\lambda') \sin(\theta/2) \qquad (2)$$

with θ the scattering angle and λ' the (reduced) wavelength of light in the solution. Peterlin[2] has adopted the Gaussian approximation to $I(\mathbf{k};t)$. It is equivalent to approximating the distribution function by the leading term of its Hermite polynomial expansion of the Nagai-Jernigan-Flory type[10-13] with the exact moments $\langle R^{2m} \rangle$. Benoit and Doty[3] have used the first two terms of the moment expansion of $I(\mathbf{k};t)$, including only $\langle R^2 \rangle$ and $\langle R^4 \rangle$. In this paper, we extend the first of these two lines to include as many higher moments as possible, since the convergence of the second is poorer. This is done by an application of the operational method developed previously by Yamakawa[13] and simplified further here, the involved operation and calculations being carried out by the use of a digital computer. We note that the other approaches cited above are difficult to improve from the point of view of successive approximations.

The method of calculation and the results are summarized in sections I and II. In section III, we discuss the determination of the mean-square radius $\langle S^2 \rangle$ of the chain and propose a method of determining M_L and λ on the basis of our $P(\theta)$ curves. In section IV, the proposed method is applied to DNA.

I. Basic Equations

The Hermite polynomial expansion of $I(\mathbf{k};t)$ may be written in the form[10-12]

$$I(\mathbf{k};t) = \exp\left(-\frac{1}{6}\langle R^2\rangle k^2\right) \sum_{m=0}^{\infty} g_{2m} k^{2m} \tag{3}$$

where

$$g_0 = 1$$

$$g_2 = 0$$

$$g_{2m} = \sum_{j=0}^{m-2} \frac{(-1)^{m-j}\langle R^2\rangle^j \langle R^{2(m-j)}\rangle}{(3!)^j\, j!\,[2(m-j)+1]!} - \frac{(m-1)\langle R^2\rangle^m}{(3!)^m\, m!} \qquad \text{for } m \geq 2 \tag{4}$$

Now we consider the characteristic function $I(\mathbf{k}|\mathbf{u}_0;t)$ when the unit vector $\mathbf{u}_0$ tangential to the chain at its initial end is fixed. From the coefficients of its moment expansion, we can obtain the moments $\langle(\mathbf{R}\cdot\mathbf{u}_0)^n\rangle$.[13] The result is given by eq 50 of ref 13, which may be rewritten as

$$\langle(\mathbf{R}\cdot\mathbf{u}_0)^n\rangle = n! \sum_{p\leq n} (2p+1)^{1/2} \sum_{\substack{\text{paths} \\ (0\to p)}} \Gamma_{0\ldots p}(t) C_\mu{}^0 \tag{5}$$

with $C_\mu{}^0 = C_\mu{}^\nu$ with $\nu_i = 0$ for all i $(1 \leq i \leq n)$. It is defined by the operator equation

$$C_\mu{}^0 = (f_p{}^0)^{-1} a_{\mu_n}{}^0 a_{\mu_{n-1}}{}^0 \ldots a_{\mu_2}{}^0 a_{\mu_1}{}^0 f_0{}^0 \tag{6}$$

where

$$f_l{}^0 = [(2l+1)/4\pi]^{1/2} \exp[-l(l+1)t] \tag{7}$$

and $a_\mu{}^0(\mu = \pm 1)$ are the creation and annihilation operators which operate on $f_l{}^0$ in such a way that

$$a_\mu{}^0 f_l{}^0 = A_{l+(1/2)(\mu-1)}{}^0 f_{l+\mu}{}^0 \tag{8}$$

with

$$A_l{}^0 = (l+1)[(2l+1)(2l+3)]^{-1/2} \tag{9}$$

$\Gamma_{0,,,p}(t)$ is the sum of the residues of the function $Q(z)$

$$Q(z) = e^{tz}/z \prod_{j=1}^{n} [z + l_j(l_j+1)] \tag{10}$$

with

$$l_j = \sum_{i=1}^{j} \mu_i \geq 0 \qquad (l_0 = 0, l_1 = 1, l_n = p) \tag{11}$$

The second sum in eq 5 is taken over all possible paths $(01l_2\cdots l_{n-1}p)$ from 0 to p in an (i, l_i)-plane, each corresponding to one of the "stone-fence" diagrams.

The characteristic function $I(\mathbf{k};t)$ may be obtained by integration of the operational expression for $I(\mathbf{k}|\mathbf{u}_0;t)$ over $\mathbf{u}_0$, and then only the paths $(0 \to 0)$ contribute. Comparison of the result with the moment expansion of $I(\mathbf{k};t)$ leads to eq 51 of ref 13 for $\langle R^{2m}\rangle$. Alternatively, a much simpler expression for $\langle R^{2m}\rangle$ may now be derived. We introduce the inverse Fourier transforms $G(\mathbf{R};t)$ and $G(\mathbf{R}|\mathbf{u}_0;t)$ of $I(\mathbf{k};t)$ and $I(\mathbf{k}|\mathbf{u}_0;t)$, respectively, and also the integral operators P and P_1

$$P = \int d\mathbf{R}$$

$$P_1 = \int_{\mathbf{u}_0 = \mathbf{e}_k} d\mathbf{R} \tag{12}$$

with $\mathbf{e}_k$ the unit vector in the direction of $\mathbf{k}$. We then have

$$P_1{}^{-1}\langle(\mathbf{R}\cdot\mathbf{u}_0)^{2m}\rangle = (\mathbf{R}\cdot\mathbf{e}_k)^{2m} G(\mathbf{R}|\mathbf{u}_0;t) \tag{13}$$

where $\langle(\mathbf{R}\cdot\mathbf{u}_0)^{2m}\rangle$ is given by eq 5 with $n = 2m$. If we take the averages of both sides of eq 13 over $\mathbf{u}_0$ with $\mathbf{e}_k$ fixed, the operator $P_1{}^{-1}$ becomes P^{-1} and then only the paths $(0 \to 0)$ contribute, so that

$$(2m)!\, P^{-1} \sum_{\substack{\text{paths} \\ (0\to 0)}} \Gamma_{0\ldots 0}(t) C_\mu{}^0 = (\mathbf{R}\cdot\mathbf{e}_k)^{2m} G(\mathbf{R};t) \tag{14}$$

Thus, recalling that

$$P(\mathbf{R}\cdot\mathbf{e}_k)^{2m} G(\mathbf{R};t) = (2m+1)^{-1}\langle R^{2m}\rangle \tag{15}$$

we obtain

$$\langle R^{2m}\rangle = (2m+1)! \sum_{\substack{\text{paths} \\ (0\to 0)}} \Gamma_{0\ldots 0}(t) C_\mu{}^0 \tag{16}$$

For a given path $(0 \to 0)$ of $2m$ steps, μ is determined uniquely, and $C_\mu{}^0$ in eq 16 is found to be

$$C_\mu{}^0 = \prod_{j=1}^{2m} A_{l_{j-1}+(1/2)(\mu_j-1)}{}^0 \tag{17}$$

with

$$\mu_1 \equiv 1$$

$$\mu_{2m} \equiv -1 \tag{18}$$

The function $Q(z)$ is also determined uniquely, and eq 10 may be rewritten in the form

$$Q(z) = e^{tz} / \prod_{j=0}^{m} [z + j(j+1)]^{p_j} \tag{19}$$

where p_j is the number of the factors with $l_i = j$ in the denominator of eq 10. The formula for residues then gives

$$\Gamma_{0\ldots 0}(t) = \sum_{\substack{j=0 \\ p_j \neq 0}}^{m} \frac{1}{(p_j-1)!} \times \left\{\frac{d^{p_j-1}}{dz^{p_j-1}}[z + j(j+1)]^{p_j} Q(z)\right\}_{z=-j(j+1)} \tag{20}$$

Finally, $\langle R^{2m}\rangle$ may be written in the form

$$\langle R^{2m}\rangle = \sum_{j=0}^{m} \sum_{i=j}^{m} A_{ij}{}^{(m)} t^{i-j} e^{-j(j+1)t} \tag{21}$$

where $A_{ij}{}^{(m)}$ are numerical constants independent of t and may be expressed in terms of $C_\mu{}^0$ and p_j, the result being omitted. Substitution of eq 21 into eq 3 completes the Hermite expansion of $I(\mathbf{k};t)$. The integral over t in eq 1 requires numerical evaluation by a computer.

II. Computer Calculations and Results

Our first problem is to calculate the coefficients $A_{ij}{}^{(m)}$. It consists of generating all possible paths $(0 \to 0)$, followed by a calculation of $C_\mu{}^0$ and a determination of p_j. This has been done on a FACOM 230-75 digital computer with a double precision of 61 binary bits at this University. One of the possible paths may be represented by a set of $\mu = \mu_1, \mu_2, \cdots, \mu_{2m}$ $(\mu_j = \pm 1)$, and *vice versa*, in which the numbers of $+1$ and -1 are the same and equal to m. All possible paths $(0 \to 0)$ may be generated by permutation of $2m$ μ_j's subject to the condition given by eq 11, the number of them being $(2m)!/m!(m+1)!$. Suppose that $2m$ μ_j's are distributed one by one in $2m$ memory boxes. If the nth $+1$ is in the α_nth memory box, the

above condition is equivalent to

$$\alpha_{n-1} < \alpha_n \leq 2n-1 \qquad (2 \leq n \leq m) \tag{22}$$

with $\alpha_1 \equiv 1$. The contributions of the two path diagrams symmetric with respect to the vertical center line are the same, and the number of paths to be actually generated may be greatly reduced. For a given μ, the calculation of C_μ^0 from eq 17 is straightforward. For a given path, p_j ($0 \leq j \leq m$) may be determined by taking $(m+1)$ memory boxes to enter +1 into the jth one if $l_i = j$ ($0 \leq i \leq 2m$), the final number of +1's in it being equal to p_j. The calculation may be further facilitated by utilizing the fact that many different paths lead to the same set of $p_0, p_1, p_2, \cdots, p_m$, and the number of different sets of the latter is only 2^{m-1} for a given m. The actual calculation of $A_{ij}^{(m)}$ has been carried out only for $m \leq 11$; this range of m has been determined from the point of view of its accuracy and necessity, as discussed below. The whole calculation from $m = 1$ to $m = 6$ has been finished in less than 2 min, and the case of $m = 11$ has taken about 8 min.

For $m = 1$, 2, and 3, the exact values of $A_{ij}^{(m)}$ can be obtained from the analytical solutions for $\langle R^{2m} \rangle$.[14-16] Thus our computer values have been found to agree with the exact values to the 17th figure. This indicates the accuracy and also the correctness of the complicated programming. For $4 \leq m \leq 11$, the accuracy may be examined in the following way. For $t \ll 1$, $\langle R^{2m} \rangle$ may be expanded in powers of t

$$\langle R^{2m} \rangle = \sum_{n=0}^{\infty} a_n t^n \tag{23}$$

with[17]

$$\begin{aligned} a_n &= 0 && \text{for } 0 \leq n \leq 2m-1 \\ &= 1 && \text{for } n = 2m \\ &= -2m/3 && \text{for } n = 2m+1 \end{aligned} \tag{24}$$

Now, a_n may be expressed in terms of $A_{ij}^{(m)}$, as seen from eq 21 and 23, and we have found that the value a_n' of a_n calculated from the computer values of $A_{ij}^{(m)}$ satisfies the inequality

$$|a_n' - a_n| < 10^{-10}|a_n'| \qquad \text{for } 0 \leq n \leq 2m+1 \tag{25}$$

Our computer values of $A_{ij}^{(m)}$ may therefore be regarded as correct at least to the 10th figure. We note that they are more accurate for smaller m. Further, although $\langle R^{2m} \rangle$ must vanish at $t = 0$, this relation does not exactly hold with the computer values; *e.g.*, $\langle R^{14} \rangle = 0(10^{-10})$, $\langle R^{18} \rangle = 0(10^{-6})$, and $\langle R^{22} \rangle = 0(10^{-3})$ at $t = 0$. Thus, the accuracy decreases with increasing m, especially at small t. In this connection, we note that Nagai[18] has obtained numerical values of $\langle R^{2m} \rangle$ as a function of t for $m \leq 20$ from the recurrence formula of Hermans and Ullman[14] by the use of a computer. His results for $m \leq 6$ are in good agreement with ours (to order 10^{-5}) for all values of t, but for higher m are much less accurate at small t.

The integration over t in eq 1 has been carried out using 24-points and 16-points Gaussian quadratures for $20 \leq L \leq 100$ and $L < 20$, respectively. These numbers of divisions have been determined to give the required accuracy such that the calculated values of $P(\theta)$ are correct to the fifth figure. Now, k^2 is less than about 10 for typical stiff chains. Therefore, the convergence of the expansion of $P(\theta)$ is necessary and sufficient in this range of k^2 for all values of L, assuming the required accuracy above. We have found that this condition may be satisfied by taking into account all moments for $m \leq 11$. The convergence is better for smaller L.

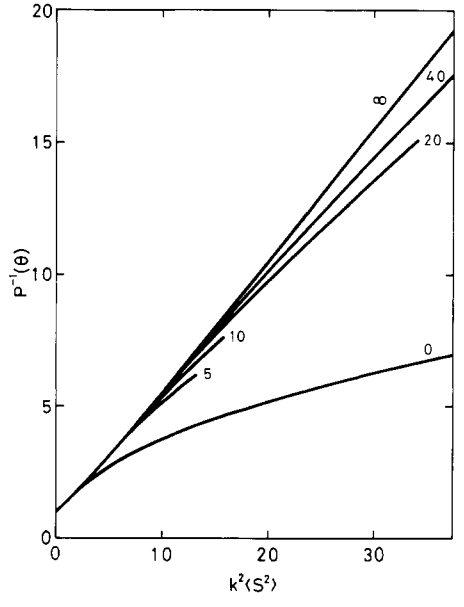

Figure 1. Values of $P^{-1}(\theta)$ plotted against $k^2\langle S^2 \rangle$. The numbers attached to the curves indicate the values of L.

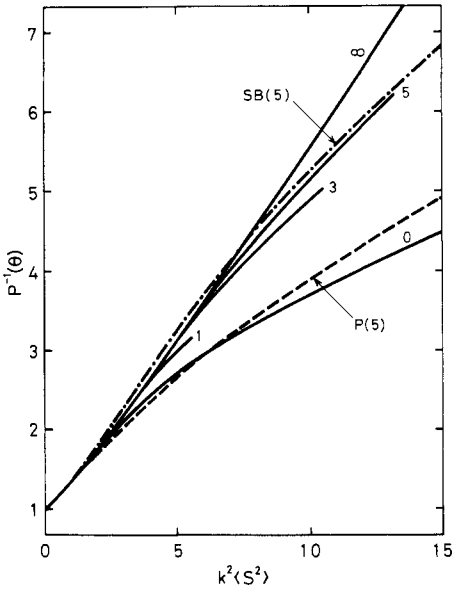

Figure 2. Values of $P^{-1}(\theta)$ in the range of small $k^2\langle S^2 \rangle$. Broken curve P represents the values calculated from the leading term of the Hermite polynomial expansion, and chain curve SB represents the values calculated from the equation of Sharp and Bloomfield.[5] The numbers attached to the curves indicate the values of L.

Figure 1 shows calculated values of $P^{-1}(\theta)$ as a function of $k^2\langle S^2 \rangle$ for various values of L, where $\langle S^2 \rangle$ is the mean-square radius of the chain of contour length L and is given by[3]

$$\langle S^2 \rangle = \frac{L}{6} - \frac{1}{4} + \frac{1}{4L} - \frac{1}{8L^2}(1 - e^{-2L}) \tag{26}$$

The numbers attached to the curves indicate the values of L; the coil (∞) and rod (0) limiting values[2,19] are also included. The curves are drawn only in the range of convergence. The domain of small $k^2\langle S^2 \rangle$ is enlarged in Figure 2. Broken curve P(5) represents the values calculated from the leading term of the Hermite polynomial expansion for $L = 5$, which are slightly different from Peterlin's original values[2] obtained by interpolation from those at $L \geq 12.5$ and $L = 0$. Chain curve SB(5) represents the correspond-

Table I
Values of $P(\theta)$ as a Function of k^2 for Various Values of L

	L										
k^2	0.5	1.0	3.0	5.0	6.0	7.0	8.0	9.0	10.0	12.5	15.0
0.5	0.9971	0.9902	0.9486	0.9025	0.8800	0.8580	0.8368	0.8163	0.7965	0.7500	0.7075
1.0	0.9942	0.9807	0.9008	0.8181	0.7799	0.7440	0.7105	0.6793	0.6501	0.5855	0.5310
1.5	0.9914	0.9712	0.8564	0.7450	0.6962	0.6519	0.6119	0.5758	0.5430	0.4738	0.4188
2.0	0.9885	0.9619	0.8150	0.6814	0.6258	0.5770	0.5341	0.4964	0.4631	0.3953	0.3437
2.5	0.9857	0.9527	0.7765	0.6261	0.5664	0.5156	0.4721	0.4347	0.4023	0.3382	0.2911
3.0	0.9829	0.9436	0.7406	0.5778	0.5161	0.4648	0.4220	0.3859	0.3551	0.2954	0.2525
3.5	0.9801	0.9347	0.7072	0.5354	0.4732	0.4226	0.3811	0.3467	0.3177	0.2624	0.2232
4.0	0.9773	0.9258	0.6761	0.4983	0.4364	0.3872	0.3474	0.3148	0.2876	0.2362	0.2003
4.5	0.9745	0.9171	0.6471	0.4656	0.4047	0.3572	0.3192	0.2884	0.2629	0.2151	0.1819
5.0	0.9717	0.9085	0.6201	0.4366	0.3773	0.3315	0.2954	0.2663	0.2423	0.1976	0.1668
5.5	0.9690	0.9000	0.5948	0.4110	0.3534	0.3095	0.2751	0.2475	0.2249	0.1830	0.1542
6.0	0.9662	0.8916	0.5713	0.3882	0.3324	0.2904	0.2576	0.2314	0.2101	0.1706	0.1436
6.5	0.9635	0.8833	0.5493	0.3678	0.3139	0.2736	0.2424	0.2175	0.1972	0.1599	0.1344
7.0	0.9607	0.8751	0.5288	0.3496	0.2976	0.2589	0.2290	0.2053	0.1860	0.1506	0.1265
7.5	0.9580	0.8670	0.5096	0.3332	0.2830	0.2458	0.2172	0.1946	0.1762	0.1425	0.1196
8.0	0.9553	0.8591	0.4916	0.3183	0.2699	0.2342	0.2067	0.1851	0.1675	0.1353	0.1135
8.5	0.9526	0.8512	0.4748	0.3049	0.2581	0.2237	0.1973	0.1765	0.1597	0.1289	0.1080
9.0	0.9499	0.8435	0.4590	0.2927	0.2474	0.2143	0.1889	0.1689	0.1527	0.1231	0.1032
9.5	0.9473	0.8358	0.4443	0.2816	0.2377	0.2057	0.1812	0.1619	0.1464	0.1180	0.09883
10.0	0.9446	0.8283	0.4305	0.2714	0.2289	0.1979	0.1743	0.1557	0.1406	0.1133	0.09487
10.5	0.9419	0.8208	0.4175	0.2620	0.2208	0.1908	0.1679	0.1499	0.1354	0.1090	0.09126
11.0	0.9393	0.8135	0.4053	0.2534	0.2134	0.1842	0.1621	0.1447	0.1306	0.1051	0.08798

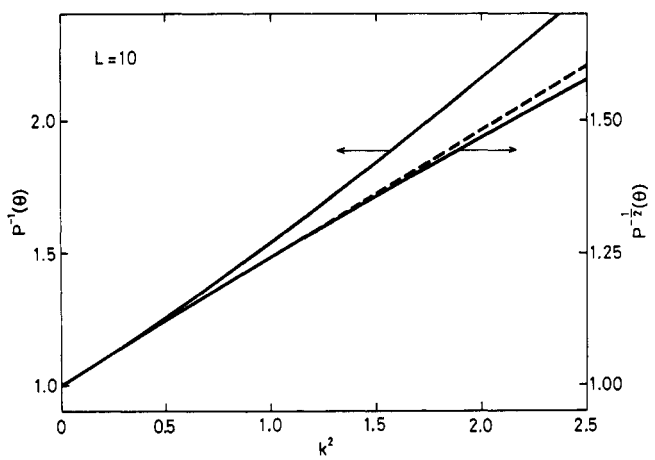

Figure 3. Comparison of the conventional and square-root plots of $P^{-1}(\theta)$ for $L = 10$. The broken line is the common initial tangent to the two curves.

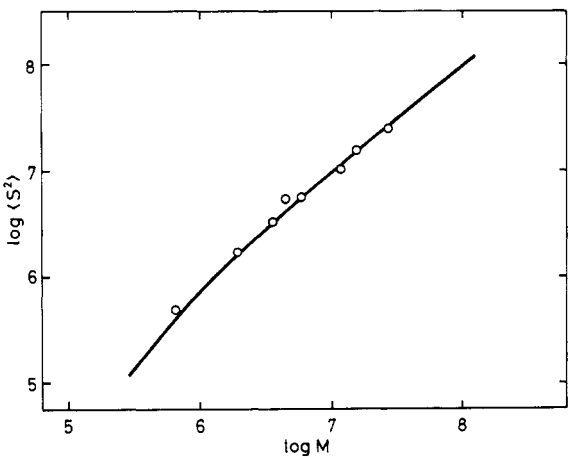

Figure 4. Double logarithmic plots of $\langle S^2 \rangle$ against M for DNA.[24] The curve represents the theoretical values with $\lambda^{-1} = 1150$ Å and $M_L = 200$ daltons/Å.

ing values calculated from the equation of Sharp and Bloomfield,[5] which has been derived using the first Daniels distribution function,[20]

$$P(\theta) = \frac{2}{x^2}(x - 1 + e^{-x}) + \frac{4}{15L} + \frac{7}{15xL} - \frac{11}{15L}e^{-x} - \frac{7}{15xL}e^{-x}$$

(Sharp-Bloomfield) (27)

with

$$x = (1/6)k^2L \tag{28}$$

It is seen that these approximate values are very poor for small L, as expected from the derivations.

However, it is interesting to note that for $L \geq 10$ and $k^2 \leq 10$, the equation of Sharp and Bloomfield gives the values which agree with ours within 1.0%, and it is useful in this range. For DNA with molecular weights less than about 2×10^6 and also other typical stiff chains, the values of $P(\theta)$ for smaller L are required. Therefore, our values of $P(\theta)$ as a function of k^2 (≤ 11) for various values of L (≤ 15) are given in Table I. The values for other values of k^2 and L may easily be obtained by interpolation.

III. Determination of M_L and λ

Before considering the problem of determining the shift factor M_L and the Kuhn segment length λ^{-1}, we make some comments on the determination of M and $\langle S^2 \rangle$. It is clear that the first coefficient of the expansion of $P(\theta)$ in powers of $\sin^2(\theta/2)$ is proportional to $\langle S^2 \rangle$, the constant of proportionality being independent of L. In the case of flexible chains ($L = \infty$), $\langle S^2 \rangle$ may be determined from the initial slope of either the conventional Zimm plot[21] of $(Kc/R_\theta)_{c=0}$ against $\sin^2(\theta/2)$ or the Berry plot[22] of $(Kc/R_\theta)^{1/2}{}_{c=0}$ against $\sin^2(\theta/2)$, where R_θ is the excess Rayleigh ratio, K is the scattering constant, and c is the concentration in conventional units. However, it is known that the latter plot gives more accurate estimates of $\langle S^2 \rangle$, especially when there are no data at small angles. From the values of $P(\theta)$ calculated from eq 27 (for $L \geq 10$) and also given in Table I, we have found that $P^{-1}(\theta)$ is linear in k^2 in the range of $P^{-1}(\theta) \lesssim 1.1$, while $P^{-1/2}(\theta)$ is linear in the range of $P^{-1}(\theta) \lesssim 1.5$ irrespective of the values of L. For illustration, the two plots for $L = 10$ are shown in Figure 3. The broken line indicates the common initial tangent to the two curves. Thus, the Berry plot is useful

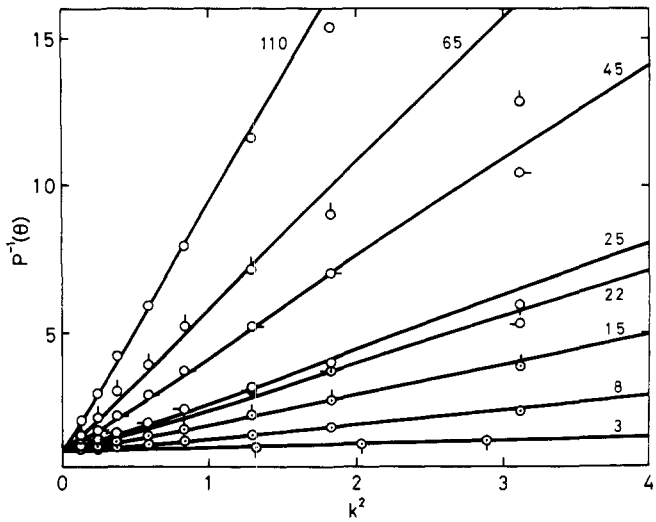

Figure 5. $P^{-1}(\theta)$ plotted against k^2 for the eight samples of DNA,[24] assuming $\lambda^{-1} = 1150$ Å. The curves are best theoretical fits to the data, and the attached numbers indicate the values of L.

Table II
Values of M_L Determined from the Plots of $P^{-1}(\theta)$ against k^2 for DNA[a]

$M \times 10^{-6}$	M_L (daltons/Å)
27.4	203–263
15.4	181–252
11.7	203–281
5.85	183–250
4.46	149–214
3.61	181–241
1.93	193–228
0.650	161–200
	Av 182–241

[a] Data obtained by Kirste.[24]

Table III
Estimates of M_L and λ^{-1} for DNA

Method	M_L (daltons/Å)	λ^{-1} (Å)
LS	200 ± 20	1150 ± 150
$[\eta] - s$[a]	195	1130

[a] See ref 1.

for the determination of $\langle S^2 \rangle$ also in the case of stiff chains, provided that data are available in the range of $P^{-1}(\theta) \lesssim 1.5$ together with the reliable intercept of the plot. The intercept, which gives the molecular weight M, may be determined from the square-root plot of $(Kc/R_\theta)_{\theta=0}$ against c. Then the determination of $P(\theta)$ is straightforward.

Now we consider our problem. For convenience, let $f(L)$ and $\langle S^2 \rangle$ be the reduced and unreduced (observed) mean-square radii, respectively, the former being given by the right-hand side of eq 26. Since $f(L) = \lambda^2 \langle S^2 \rangle$, and L is given by

$$L = \lambda M / M_L \tag{29}$$

we have the relations

$$\log f(L) = \delta_1 + \log \langle S^2 \rangle \tag{30}$$

$$\log L = \delta_2 + \log M \tag{31}$$

with

$$\delta_1 = 2 \log \lambda \tag{32}$$

$$\delta_2 = \log (\lambda / M_L) \tag{33}$$

Equations 30 and 31 suggest that the curve of log $f(L)$ plotted against log L may be displaced by δ_1 in the ordinate direction and by δ_2 in the abscissa direction to fit experimental plots of log $\langle S^2 \rangle$ against log M on the same scale. With these displacements, M_L and λ may be determined from eq 32 and 33. However, this procedure leads to only rough estimates of them, and the more precise determination may be achieved using angular data for $P(\theta)$ in addition to data for $\langle S^2 \rangle$.

If we assign some value to λ, we can plot observed values of $P^{-1}(\theta)$ against k^2, since

$$k = (4\pi / \lambda\lambda') \sin(\theta/2) \tag{34}$$

with λ' the unreduced wavelength in the medium. Thus, we may use the value of λ obtained from the above logarithmic plot of $\langle S^2 \rangle$ against M and determine L in such a way that the theoretical curve of $P^{-1}(\theta)$ plotted against k^2 for that L is a best fit to the experimental plot. With these values of λ and L, we may determine M_L from eq 29. If values of M_L thus determined for all samples do not agree, we take the average. If it is different from the value of M_L determined by the first procedure (eq 30–33), we reestimate λ and M_L by the first procedure and repeat the analysis until the coincidence is attained.

Although Peterlin[2] and Geiduschek and Holtzer[23] have used plots of $P^{-1}(\theta)$ against $k^2\langle S^2 \rangle$ and log $k^2\langle S^2 \rangle$, respectively, these plots are insensitive to the change in λ or M_L, and cannot be used for our purpose.

IV. Application to DNA

Although M_L is known to be 195 daltons/Å for DNA, we apply the procedure proposed above to DNA, assuming that its M_L is unknown. For this purpose, we use the data obtained by Kirste.[24] We have first reestimated M, $\langle S^2 \rangle$, and $P(\theta)$ from his raw data according to the proposed procedure with the use of the value of 0.168 (ml/g) for the specific refractive index increment. The values of M are close to his original values.

Figure 4 shows double logarithmic plots of $\langle S^2 \rangle$ (in Å^2) against M. The possible value of λ^{-1} determined from eq 32 is 1000–1300 Å, and the corresponding value of M_L determined from eq 33 is 170–220 daltons/Å. Values of $P^{-1}(\theta)$ ($12° \leq \theta \leq 60°$) for the eight samples differing in M are plotted against k^2 for $\lambda^{-1} = 1150$ Å in Figure 5, where the curves represent the theoretical values and the numbers attached to them indicate the values of L. Each of these curves is a best fit to the data. The data at high angles are seen to deviate from the curves. This is probably due to the polydispersity of the samples. The possible range of λ^{-1} above leads to some ranges of the values of L and therefore M_L determined from the plots of Figure 5. The ranges of M_L thus determined are given in Table II together with the average range. From a comparison of this range of M_L and that determined above from eq 33, we may conclude that $M_L = 200 \pm 20$ daltons/Å. Thus the curve in Figure 4 represents the theoretical values with $\lambda^{-1} = 1150$ Å and $M_L = 200$ daltons/Å. In Table III, these estimates of M_L and λ^{-1} are compared with those obtained previously[1] from a combination of viscosity and sedimentation ($[\eta] - s$). There is seen to be good agreement between them.

In conclusion, it must be noted that M_L and λ^{-1} can be determined from the combination of viscosity and sedimentation data more accurately than from light-scattering data. In order to obtain the more precise estimates from

the latter, a study of the effect of polydispersity is required.

Acknowledgment. We thank the Ministry of Education of Japan for the grant-in-aid for scientific research in the 1973 academic year. We are also grateful to Professor R. G. Kirste of the University of Mainz, who kindly sent us his light-scattering data for DNA.

References and Notes

(1) H. Yamakawa and M. Fujii, *Macromolecules*, **7**, 128 (1974).
(2) A. Peterlin, *J. Polym. Sci.*, **10**, 425 (1953); "Electromagnetic Scattering," M. Kerker, Ed., Pergamon Press, London, 1963, p 357.
(3) H. Benoit and P. Doty, *J. Phys. Chem.*, **57**, 958 (1953).
(4) J. E. Hearst and R. A. Harris, *J. Chem. Phys.*, **46**, 398 (1967).
(5) P. Sharp and V. A. Bloomfield, *Biopolymers*, **6**, 1201 (1968).
(6) H. Yamakawa, *Annu. Rev. Phys. Chem.*, in press.
(7) J. A. Harpt, A. I. Krasna, and B. H. Zimm, *Biopolymers*, **6**, 595 (1968).
(8) J. B. Hays, M. E. Magar, and B. H. Zimm, *Biopolymers*, **8**, 531 (1969).
(9) C. W. Schmid, F. P. Rinehart, and J. E. Hearst, *Biopolymers*, **10**, 883 (1971).
(10) K. Nagai, *J. Chem. Phys.*, **38**, 924 (1963).
(11) R. L. Jernigan and P. J. Flory, *J. Chem. Phys.*, **50**, 4185 (1969).
(12) P. J. Flory, "Statistical Mechanics of Chain Molecules," Interscience, New York, N. Y., 1969, p 397.
(13) H. Yamakawa, *J. Chem. Phys.*, **59**, 3811 (1973).
(14) J. J. Hermans and R. Ullman, *Physica*, **18**, 951 (1952).
(15) G. Porod, *J. Polym. Sci.*, **10**, 157 (1953).
(16) S. Heine, O. Kratky, G. Porod, and P. J. Schmitz, *Makromol. Chem.*, **44-46**, 682 (1961).
(17) H. Yamakawa and M. Fujii, *J. Chem. Phys.*, **59**, 6641 (1973).
(18) K. Nagai, *Polym. J.*, **4**, 35 (1973).
(19) P. Debye, *J. Phys. Colloid Chem.*, **51**, 18 (1947).
(20) H. E. Daniels, *Proc. Roy. Soc. Edinburgh. Sect. A*, **63**, 290 (1952).
(21) B. H. Zimm, *J. Chem. Phys.*, **16**, 1099 (1948).
(22) G. C. Berry, *J. Chem. Phys.*, **44**, 4550 (1966).
(23) E. P. Geiduschek and A. Holtzer, *Advan. Biol. Med. Phys.*, **6**, 431 (1958).
(24) R. G. Kirste, *Discuss. Faraday Soc.*, **49**, 51 (1970).

Polyelectrolytes in Salt Solutions. Quantitative Separation of Binding and Electrostatic Effects for Poly(L-ornithine) and Poly(L-lysine)

G. Conio, E. Patrone, G. Rialdi, and A. Ciferri*

Istituto di Chimica Industriale, University of Genoa, Genoa, Italy. *Received January 29, 1974*

ABSTRACT: Potentiometric titrations for poly(L-ornithine) (Orn_n), calorimetric measurements for Orn_n and poly-L-lysine (Lys_n), and optical rotatory dispersion data for Orn_n and Lys_n are presented. Measurements were performed in the presence of variable quantities (up to 2 *M*) of KSCN and KCl. In agreement with previous findings, KSCN causes stabilization of the helical conformation for Lys_n, even when the polymer is fully ionized (pH 3). Negligible helix formation is instead observed for Orn_n. KCl is unable to induce helix formation for both Lys_n and Orn_n (pH 3). These results have been quantitatively interpreted in terms of an extension of existing formalisms of the electrostatic free energy of polyions in salt solutions. The modification introduced accounts for a reduction of the fixed charge on the polymer caused by a binding reaction between charged ϵ-amino residues and SCN^- ions. The binding reaction is formulated in terms of multiple equilibria theory. Classical effects of the ionic strength on the slopes of pK_{app} *vs.* *Z* plots and on intrinsic equilibrium constants were retained. The satisfactory agreement between experimental data and theoretical predictions strongly supports the validity of the model based on the simultaneous occurrence of specific (binding) and nonspecific (electrostatic) interactions for polar solutes in salt solutions.

Salts affect the conformational properties of polyelectrolytes by contributing to the charge-dependent and to the charge-independent part of the free energy. When the charge density of the polymer is high, a prevailing contribution of the electrostatic free energy is expected. If the surface potential of the macroion can be estimated, salt effects may be predicted according to different models.

Simple electrostatic effects, *i.e.*, charge screening according to the Debye–Hückel concept, have been theoretically described for a variety of macroion models.[1] The concept of ion condensation[2,3] has been recently introduced in a model for the conformational transition of rodlike polyelectrolytes possessing high charge density.[4] According to this theory, some counterions must "condense" on the surface of the rod when the charge density reaches a critical value, specifically during the random coil → helix transition.

On the other hand, it has been shown that salts may affect conformational stability by interactions which are not readily interpreted in terms of charge screening, or ion condensation effects.[5] For instance, Puett *et al.*[6-8] have reported that a conformational transition from coil to helix is observed for fully charged poly(L-lysine) when KSCN is added to the solution (the transition was not induced in the presence of comparable amounts of KCl). Further work[9] has shown that the role of ion type is evident for every value of the degree of ionization. This result parallels the observed deviations (from the traditional model) of the colligative properties of acidic polyelectrolytes in the presence of certain divalent cations.[2] These effects cannot be rationalized by purely electrostatic models and require consideration of other specific properties of the counterions.

The ion binding concept has been often advocated in order to describe specific properties of ions.[5] Ion binding effects should occur simultaneously with screening effects associated with "free" (*i.e.*, unbound) coions and counterions. We have often stressed[10,11] that the ability which some ions (*i.e.*, SCN^-, Li^+, etc.) have to bind to polar substrates (*i.e.*, peptide bonds) should also be manifested with polyelectrolytic solutes. However, quantitative verifications of the validity of the ion binding mechanism for altering the conformational stability of polyelectrolytes (when multiple equilibria effects cannot be neglected) have not been forthcoming.

In the present paper, we attempt to describe quantitatively the titration and the calorimetric behavior of poly(L-ornithine) and poly(L-lysine), and the KSCN-induced transition for the latter, in terms of binding and screening effects.